

## GLOBAL DISTRIBUTION OF AURORAL PROTON PRECIPITATION INFERRED FROM THE DMSP DATA

O.I. Yagodkina, V.G. Vorobjev (*Polar Geophysical Institute, Apatity, Murmansk region*)

**Abstract.** For the further development of the Auroral Precipitation Model (<http://apm.pgia.ru/>), which yields global patterns of electron precipitation, the global model of ion (proton) precipitation is developed by using the same database of DMSP F6 and 7 spacecraft. Global distributions of the average precipitating proton energy and proton energy flux in the different MLT sectors were simulated in dependence on the magnetic activity expressed by AL and Dst. It is shown that maximum of the proton energy flux occurs in the afternoon (15-18 MLT) in DAZ, where at AL = -1000 nT the proton flux exceeds the electron one in ~3.5 times. In AOP the value of the proton flux decreases with the increasing of magnetic activity. The maximum of proton energy is registered in AOP during daytime hours of MLT. In DAZ the maximum of proton energy is observed in the afternoon. It is shown a good correlation of the calculated and observed by DMSP F6, F7 and F9 precipitation patterns during two strong magnetic storms of February 8–9, 1986, and March 13–14, 1989 with Dst = ~ -300 and ~ -600 nT, respectively. The model will allow us to calculate the total ionosphere conductivities and total precipitation power depending on the magnetic activity level.

### Introduction

The features of the ion (proton) precipitation and the global pattern of the energy proton input were examined by many researches. Studies based on particle and optical measurements (Akasofu, 1974; Feldstein and Galperin, 1985; Hardy et al., 1989; Gussenhoven et al., 1987) have shown the existence of a region of diffuse aurora (ion precipitation) equatorward of the discrete aurora (electron precipitation) in the dusk-midnight sector. The first statistical model of auroral ion precipitation was published by Hardy et al., 1989. In their investigations the global proton precipitation patterns have been statistically described as a function of the Kp geomagnetic index based on several years of ion energy spectra measurements by the DMSP satellites. They indicate that the maximum energy flux occurs in C-shaped regions symmetric about a meridian running pre-noon to pre-midnight. In comparison to the DMSP statistical electron precipitation data (Hardy et al., 1985), the statistical proton oval is displaced equatorward of the electron oval in the afternoon and pre-midnight sectors, although some overlap is frequently observed. As a result, the model was presented in the plots of selected isocontours of the integral number flux and average energy as a function of magnetic local time and corrected geomagnetic latitude for Kp-index.

Studies of Basu et al., 1987; Senior et al., 1987; Lilensten and Galand, 1998, relying on incoherent scatter radar measurements and simultaneous satellite observations showed that protons were the main source of ionization in afternoon and pre-midnight sectors at the equatorial edge of the auroral oval.

Investigations of the morphology and dynamics of the proton aurora with SI12 images (Immel et al., 2002; Burch et al., 2002) have revealed the presence of detached subauroral proton arcs in the afternoon and dusk sectors of the Northern Hemisphere under changing interplanetary magnetic field (IMF) conditions. Remote sensing of the proton aurora characteristics from IMAGE-FUV was examined by Bisikalo et al., 2003. According to their investigation the proton precipitation in proton-dominated auroral structures frequently observed in the afternoon and pre-midnight sectors at the latitudes equatorward of the auroral oval. They belong to two categories of proton auroral features: (i) hydrogen arcs known to occur in the evening sector equatorward of the electron oval and (ii) detached proton arcs observed with IMAGE-FUV in the afternoon sector following changes in orientation of the interplanetary magnetic field.

Our results are based at the immediate data using DMSP F6 and F7 spacecraft observations of the average ion energy and energy fluxes in different precipitation regions. In order to investigate the ion (proton) characteristics, we have used early our created the Auroral Precipitation Model (<http://apm.pgia.ru/>) which allows to receive boundary locations of different types of auroral precipitation at the different levels of magnetic activity (AL and Dst indexes) and will also to receive the planetary picture of average proton energies and fluxes in different precipitating zones.

### Data used and analysis

To carry out studies of the characteristics of precipitating protons within two auroral regions (DAZ – the diffuse auroral zone and AOP - the auroral oval precipitation), we used a database of the data from the DMSP F6 and DMSP F7 spacecraft over an entire year (1986), including approximately 35 000 passes in all sectors of local geomagnetic time. The following boundary locations were used: on the nightside in the DAZ region the proton energy input was determined between b1i – b2i boundaries where b1i is the 'zero-energy' proton boundary; b2i is the point where the energy flux of protons above 3 keV has a maximum; the AOP region is divided on the equatorward (b2i – b4s) and the poleward (b4s–b5i) areas. The b4s is the structured/unstructured boundary, based on the running average of correlation coefficients between individual electron spectra and their neighbors. The b5i is

the poleward boundary of the auroral oval as determined by an abrupt drop in the proton energy flux. The dayside proton boundaries coincide with the dayside electron boundaries. Here and hereinafter we conceded the average energy fluxes and the average energies rate over the AOP region which on the nightside includes area between b2i - b5i.

The average energy and the number flux of protons between the precipitation boundaries in all magnetic local time sectors were calculated. The regression equations used for study of the behavior the proton precipitation for different level of magnetic activity.

In Fig. 1 the average proton energy fluxes and the energies integrated over each MLTs in the DAZ and AOP regions are plotted as a function of the magnetic activity expressed by the AL – index.

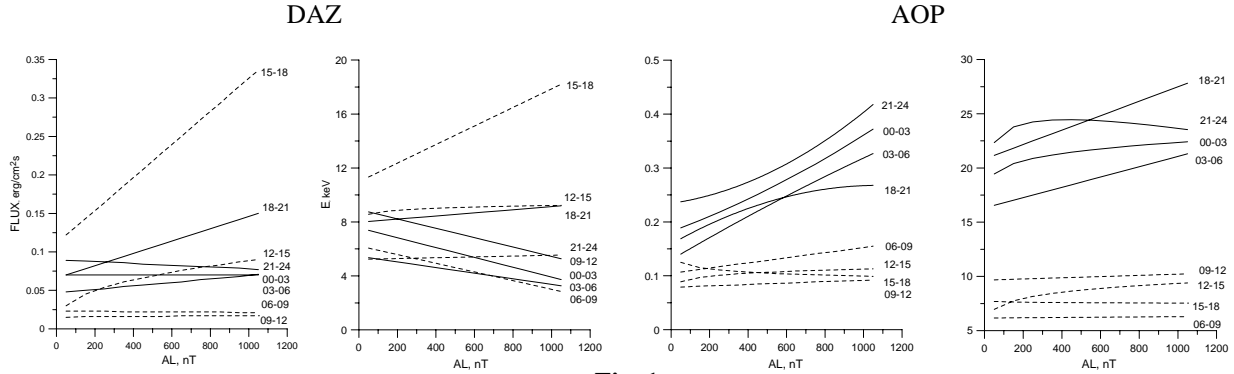


Fig. 1

The energy fluxes and energies in the nightside MLTs (00-03, 03-06, 18-21, 21-24) are marked by the solid lines, in the dayside MLTs (06-09, 09-12, 12-15, 15-18) those are marked by the dashed lines.

**DAZ region:** In the afternoon sectors (12-15, 15-18, 18-21 MLTs) the proton precipitating fluxes grow with increasing activity and have the maximum in the 15-18 MLT. In the prenoon sectors (06-09, 09-12 MLTs) the fluxes do not change with the increasing activity, and in the pre-midnight and post-midnight sectors (21-24, 00-03, 03-06 MLTs) the values of the fluxes vary weakly with increase of activity. The maximum energies have the same tendency in the afternoon MLTs but in the other sectors the average proton energies either decrease or do not vary according to the magnetic activity.

**AOP region:** The maximum proton fluxes and energies occur in the nightside MLTs. The energies and the fluxes in the dayside sectors vary weakly.

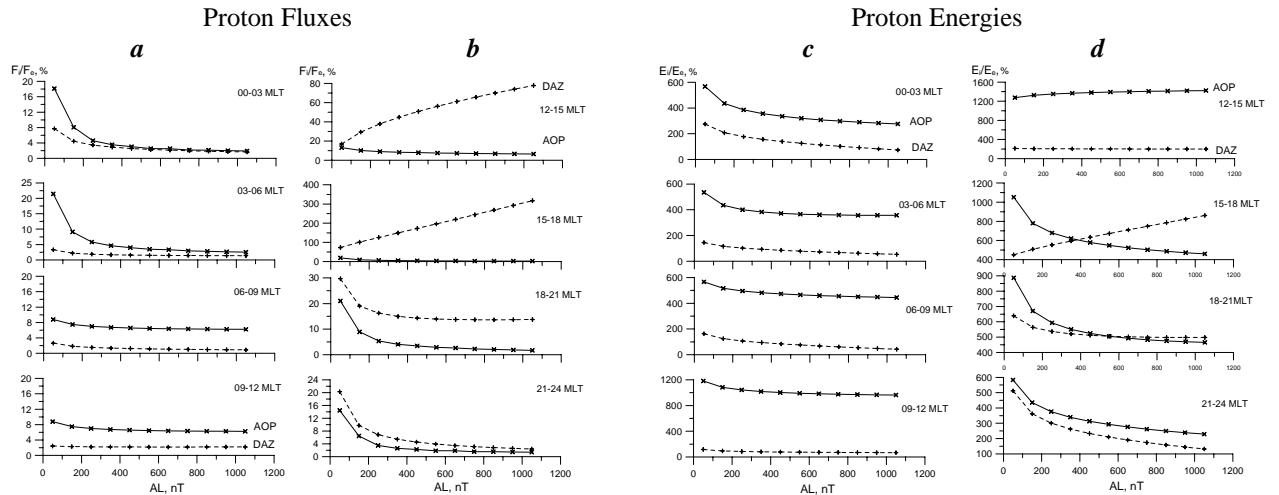


Fig. 2

Fig. 2 demonstrates the ratio of the proton fluxes to the electron fluxes  $F_i/F_e$  (a,b) and the proton energy to the electron energies  $E_i/E_e$  (c,d) depending on the magnetic activity over eight MLTs. The inspection of the  $F_i/F_e$  shows that in the DAZ the intensity of proton precipitation gains with the increasing activity in the afternoon 12-15 and 15-18 MLTs. A significant portion of protons takes place in the 15-18 MLT. In this sector during quiet condition (AL~50-150 nT) the electron precipitating fluxes exceeds proton precipitation. However the proton precipitation exceeds the electron one ~ in 3.5 times when AL= - 1000 nT. In all other sectors the ratio of the fluxes

drops with the increase of activity. The activity curves drop in the AOP region in all MLTs with the increasing activity.

Fig. 2c,d shows the ratio of the proton energies to the electron energies. In the both zones in the prenoon MLT (c) the ratio drops with the increase of the magnetic activity. The same tendency remains in the 18-21 and 21-24 MLTs. In the 12-15 MLT the ratios do not vary with the increasing activity and in the 15-18 MLT the energy of protons increases in the DAZ and decreases in the AOP with the increasing  $|AL|$ .

The variations of the ratio of proton fluxes to the electron fluxes and the proton energies to the electron energies depending on the MLT and the magnetic activity are presented in the Fig. 3a,b. The ratios in the DAZ are presented on the upper panel, in the AOP – on the bottom. As seen from the Figure the maximum proton fluxes occur in the DAZ in the afternoon and the ratio gains about in 4 times when the magnetic activity increases from  $AL = -50$  nT up to  $AL = -1000$  nT. In the AOP the contribution of proton fluxes decreases with the increasing activity. Fig. 3b illustrates the behavior of the ratio of the energies within the DAZ and AOP. In the DAZ the peak of the ratio sets in the 18-21 MLT during the quiet conditions and shifts to 15-18 MLT sector during the disturbed conditions ( $AL = -1000$  nT). In the AOP the peak of the ratio sets in the daytime and the ratio in the prenoon hours depends on the magnetic activity weakly. In the afternoon the ratio drops with the increasing activity.

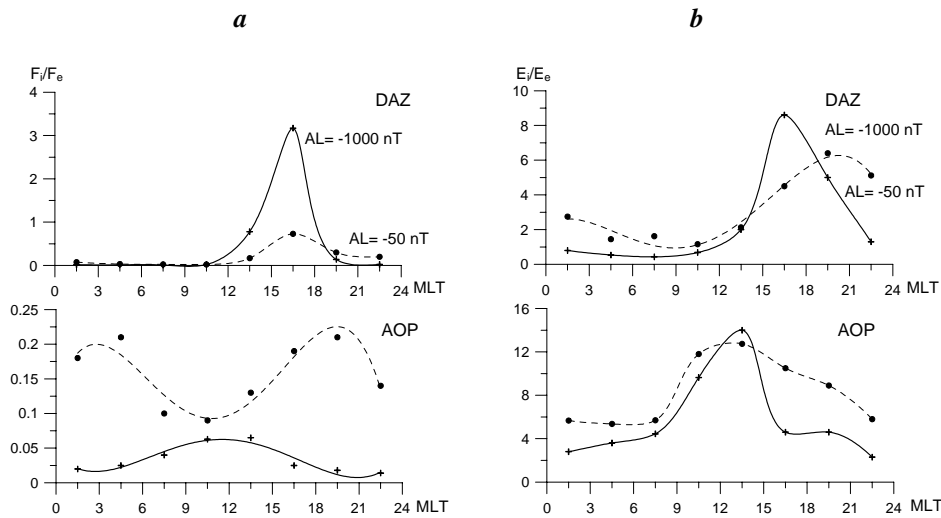


Fig. 3

The comparison of the electron and the proton auroral precipitation for  $AL = -100$  nT and  $AL = -1000$  nT is illustrated in Fig. 4a,b. As can see from the Figure the auroral precipitation demonstrates the maximum electron fluxes and energies in the AOP region during night hours, the minimum fluxes are registered in the region of the noon. In the DAZ region the maximum electron flux occurs in the morning (03-06) and it's minimum in the afternoon (15-18). In 15-18 MLT the proton fluxes have peak value which increases by approximately a factor of 2.5 from  $0.13 \text{ erg/cm}^2\text{s}$  to  $0.33 \text{ erg/cm}^2\text{s}$  when the  $AL$ - index changes from  $-100$  nT up to  $-1000$  nT. Thus a clear pattern of anticorrelation exists between regions of strong electron and proton precipitation. Different distribution of particles in the locations and times we can see in the behavior of electron and proton energies within DAZ.

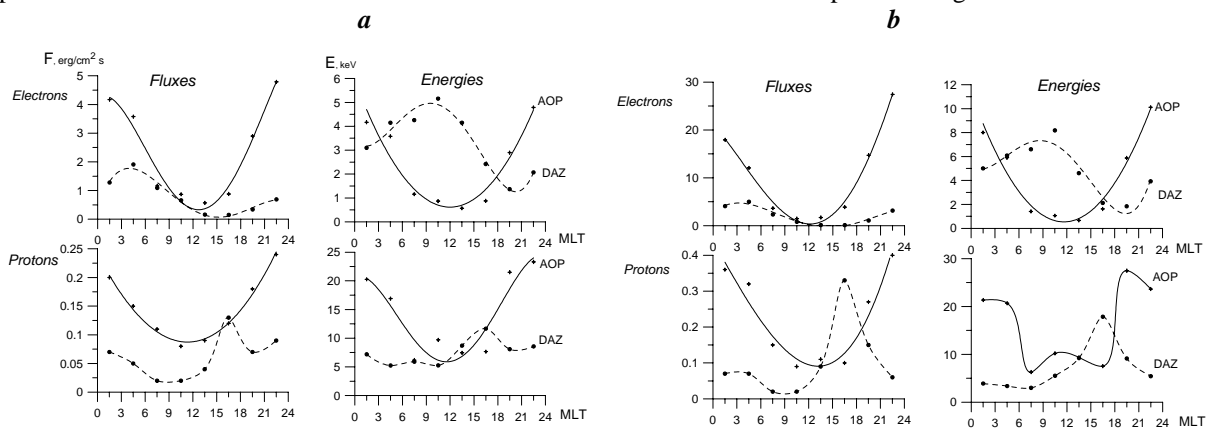


Fig. 4

The maximum value of electron energy occurs in pre-noon (09-12) and slowly falls down to the evening (18-21). The peak of proton energy is situated in the after-noon (15-18) and its value varies from about 12 keV to 18 keV with the magnetic activity grow. Thus, the maximum proton energy concentrates in the afternoon and pre-midnight sectors in the DAZ, at the equatorial edge of the auroral oval.

We compared the proton precipitation from DMSP F6, F7 and F9 spacecraft data and those obtained by means of the empirical formulas for two magnetic storms on February 8–9, 1986 (18-21, 21-24 MLTs), and March 13–14, 1989 (21-24 MLT), with a Dst value at a maximum of approximately –300 and –600 nT, respectively. The energy proton input (average flux and energy) within the DAZ (b1i – b2i) and AOP (b2i – b4s, b4s – b5i) was estimated from the model regression equations and compared with DMSP spacecraft data. The scatter in the DMSP data was very large in the DAZ region and reduced in the poleward part of the AOP. The empirical formulas give the close approximation in the poleward part of the AOP. Under large scatter of the experimental data the model regression equations allow to obtain information about the energy input of proton precipitation. The model describes well enough the global distribution of the auroral proton precipitation during the magnetic storms of different intensity and the model calculations are capable of filling the gaps in spacecraft measurements.

## Conclusion

Early obtained the database from the DMSP F6 and DMSP F7 spacecraft data was used to examine the proton precipitation in all sectors of local geomagnetic time. While electrons are the dominant particle energy source in the auroral precipitation, proton precipitation inputs a considerable part in the afternoon and pre-midnight sectors. The maximum proton precipitation was found in DAZ equatorward of the auroral oval. The enhancement of the proton fluxes and energies is registered with the increasing magnetic activity. The proton precipitation exceeds the electron precipitation during the disturbed conditions. The comparison of the calculated and the experimental data during two magnetic storms illustrates that model calculations could be used for filling gaps in spacecraft measurements especially during large magnetic storms when the spacecraft data are no available.

**Acknowledgement.** This work was supported by RFBR grant 12-05 -00273a and Programs 4 and 22 of the RAS Presidium.

## References

- Akasofu, S-I.: Discrete, continuous and diffuse auroras, *Planet. Space. Sci.*, 22, 1723, 1974.
- Basu, B., J.R. Jasperse, R.M. Robinson, R.R. Vondrak, and D.S. Evans, Linear transport theory of auroral proton precipitation: a comparison with observations, *J. Geophys. Res.*, 92, 5920, 1987.
- Bisikalo D.V., V.I. Shematovich, J.-C. Gerard, M. Meurant, S.B. Mende, and H.U. Frey, Remote sensing of the proton aurora characteristics from IMAGE-FUV, *Annales Geophysicae*, 21, 2165–2173, 2003.
- Burch, J.L., Lewis, W.S., Immel, T.J., Anderson, P.C., Frey, H., Fuselier, S.A., Gerard, J.C., Mende, S.B., Mitchell, D.G., and Thomsen, M.F.: Interplanetary Magnetic field control of afternoon sector detached auroral arcs, *J. Geophys. Res.*, 107, 1251, 10.1020/2001JA007554, 2002.
- Feldstein, Y.I. and Galperin, Y.I.: The auroral luminosity structure in the High-Latitude Upper atmosphere: Its dynamics and relationship to the large-scale structure of the Earth's magnetosphere, *Rev. of Geophys.*, 23, 217, 1985.
- Gussenhoven, M.S., Hardy, D.A., and Heinemann, N.: The equatorward boundary of auroral ion precipitation, *J. Geophys. Res.*, 94, 3273, 1987.
- Hardy D.A., M.S. Gussenhoven, and E. Holeman, A statistical model of auroral electron precipitation, *J. Geophys. Res.*, 90, A5, 4229-4248, 1985.
- Hardy D.A., M.S. Gussenhoven, and D. Brautigan, A statistic model of auroral ion precipitation, *J. Geophys. Res.*, 94, 370-392, 1989.
- Immel, T.J., Mende, S.B., Frey, H.U., Peticolas, L.M., Carlson, C.W., Gerard, J.C., Hubert, B., Fuselier, S., and Burch, J.L.: Precipitation of auroral protons in detached arcs, *Geophys. Res. Lett.*, 29, 10.1029/2001GL03847, 2002.
- Lilensten J. and M. Galand, Proton-electron precipitation effects on the electron production and density above EISCAT (Tromso) and ESR, *Ann. Geophysicae* 16, 1299-1307, 1998.
- Senior, C., J.R. Sharber, O. de la Beaujardiere, R.A. Heelis, D.S. Evans, J.D. Winningham, M. Sugiura and W.R. Hoegy, E and F region study of the evening sector auroral oval: a Chatanika/Dynamics Explorer2/NOAA6 comparison, *J. Geophys. Res.*, 92, 2477, 1987.